Vol. **111** (2007) *ACTA PHYSICA POLONICA A* No. 2

Atomic Force Microscopy and Quartz Crystal Microbalance Study of the Lectin–Carbohydrate Interaction Kinetics

K. Lebed[a], A.J. Kulik[b], L. Forró[b] and M. Lekka[a]

[a]The Henryk Niewodniczański Institute of Nuclear Physics
Polish Academy of Sciences, Radzikowskiego 152, 31-342 Kraków, Poland
[b]The Institute of Physics of Complex Matter
Ecole Polytechnique Fédérale de Lausanne (EPFL)
1015 Lausanne, Switzerland

(Received May 18, 2006; revised version January 10, 2007)

Two analytical methods, atomic force microscopy and quartz crystal microbalance, were applied to the study of the reaction kinetics occurring between concanavalin A and carboxypeptidase Y, presenting the specific lectin–carbohydrate recognition. The dissociation rate constants for concanavalin A–carboxypeptidase Y complex obtained using both atomic force microscopy and quartz crystal microbalance were of the same order of magnitude: $k_{\rm diss} = 0.170 \pm 0.060\ {\rm s}^{-1}$ and $k_{\rm diss} = 0.095 \pm 0.002\ {\rm s}^{-1}$, respectively. In addition, each method alone aided in determining other parameters characterizing the studied interaction. Quartz crystal microbalance permitted us to estimate the association rate ($k_{\rm ass} = (5.6 \pm 0.1) \times 10^4\ {\rm M}^{-1}\ {\rm s}^{-1}$) and the equilibrium ($K_{\rm a} = (0.59 \pm 0.01) \times 10^6\ {\rm M}^{-1}$) constants for the binding process occurring between concanavalin A and mannose residues of carboxypeptidase Y under given experimental conditions. Atomic force microscopy in force spectroscopy mode enabled the determination of the energy barrier position of $r = 2.29 \pm 0.04$ Å characterizing the dissociation of concanavalin A–carboxypeptidase Y molecular complex. The presented results show that both atomic force microscopy and quartz crystal microbalance can be used to determine quantitative parameters characterizing the specific molecular interaction. Both methods can be easily combined for complementary and/or alternative studies of a chosen molecular interaction. By preparing the samples in the same manner the direct comparison between the data obtained via atomic force microscopy and quartz crystal microbalance can be made.

PACS numbers: 87.64.Dz, 84.37.+q, 87.15.Kg, 82.37.Np, 81.65.Cf, 52.77.Bn

1. Introduction

The important characteristics of the biological molecule interactions are the kinetic parameters and the equilibrium constants of the studied reaction. Typically, specific interactions between the biological molecules are studied using a number of commonly known physical and biochemical methods, such as surface plasmon resonance (SPR) [1], enzyme linked immunosorbent assay (ELISA) [2], analytical affinity chromatography (HPLAC) [3], affinity capillary electrophoresis (ACE) [4], etc. Some methods determine only the affinity of studied species, while others also provide information about the kinetics of the interaction.

Among the above-mentioned methods, atomic force microscopy (AFM) and quartz crystal microbalance (QCM) could also be listed. AFM in its force spectroscopy mode allows the determination of the dissociation rate constant and the position of the transition state of the energy barrier characterizing the dissociation process of the studied molecular complex [5, 6]. QCM also enables the estimation of the dissociation rate constant as well as the equilibrium and association rate constants of molecular interactions [7–9]. Such AFM or QCM experiments are carried out in liquid, using immobilized receptor molecules, whereas the used ligands may be either free in solution (for QCM measurements) or immobilized on the probe tip (for AFM measurements). The molecules of interest are not labelled and are immobilized according to the similar procedures for both AFM and QCM experiments. Thus, it is reasonable to suggest that the results obtained by these two methods should be comparable.

The present work is a continuation of our previous AFM and QCM studies [10, 11] of the specific lectin–carbohydrate interaction between the pair of proteins carboxypeptidase Y (CaY) and concanavalin A (Con A). CaY is a glycoprotein containing the mannose type of ligand specifically recognized by the lectin concanavalin A. The high affinity of Con A to specific sugar residues is useful not only for characterization of malignant cells [12], but also in different types of bioassays for studying the glycoprotein and carbohydrate recognition processes [13, 14]. Our previous AFM study has shown the successful identification of the specific Con A–CaY interaction by means of force spectroscopy [10]. The first aim of the present paper is the dynamic force spectroscopy study of the Con A–CaY complex dissociation and, consequently, obtaining the dissociation rate constant and the position of the energy barrier characterizing the studied dissociation process. The other aim of the work is to use these quantitative parameters together with the equilibrium binding constant obtained using the QCM technique for the characterization of the energy landscape of the dissociation path of the Con A–CaY complex. The detailed QCM study of the kinetic properties of the CaY binding to immobilized Con A has been published in [11], while the present work shows only the main aspects of that study. One more important aim of the work was to compare the values of the dissociation rate obtained using both AFM and QCM measurements.

It is worth mentioning that in the force spectroscopy mode of AFM, while successively approaching and retracting the AFM tip with immobilized ligands to the receptor-modified surface, data were recorded as force–distance curves. These curves reflect the forces interacting between the tip and the surface. The important thing is to select exactly the type of curve that corresponds to the specific interaction between ligand and receptor molecules and to omit other types that reflect non-specific interactions. The proper selection of force–distance curves provides the experimental accuracy that is extremely important for AFM applications as a biosensor technique.

In the present work, a method for simplifying the force–distance curve selection was used. It was suggested that if distinct molecules were put in some specific order on a micro-area of surface, then the force spectroscopy data obtained from such a prepared substrate would be spatially separated in the same order, which would facilitate the selection of the correct data (see Sect. 3.1). The protein patterning was performed using poly(dimethylsiloxane) (PDMS) stamps with a micro-pattern on their surfaces [10, 15].

2. Materials and methods

2.1. Materials

The proteins Con A (concanavalin A from *Canavalia ensiformis*, Jack Bean, Type VI), fluorescein isothiocyanate labeled Con A (Con A-FITC), CaY (carboxypeptidase Y from *Baker's Yeast*) and BSA (bovine serum albumin) were purchased from Sigma. Tris buffered saline (TBS), 50 mM Tris-HCl, 150 mM NaCl was purchased from Fluka. For recognition measurements, the TBS buffer was supplemented with 1 mM concentration of $MgCl_2$, $MnCl_2$, and $CaCl_2$, since the presence of these ions is essential for binding activity of Con A [16]. All solutions were prepared using deionized water (18.2 MΩ cm).

2.2. Protein immobilization

The proteins were immobilized either on the surface of a glass coverslip used in AFM measurements or on the surface of gold electrodes of the quartz crystal utilized in QCM measurements. Both procedures for protein immobilization were similar for all the substrates and they have been described elsewhere in detail [10, 11, 17]. The schematic diagram for them is presented in Fig. 1.

Briefly, after thorough cleaning, both studied surfaces were enriched with amine-groups. The glass surface was silanized using 3-aminopropyltriethoxysilane (APTES, Sigma) while the gold surface was treated with 4-aminothiophenol (4-ATP, Sigma). Next, the substrates were incubated in a 2.5% glutaraldehyde solution for 20 min. After these treatments the aldehyde groups present on the substrate surface readily bound amine-groups of proteins via the strong covalent bonds (the Schiffs reaction). Then 2.5 μM protein solutions (Con A, Con A-FITC or BSA) were applied. Glass coverslips were coated with proteins via PDMS stamps [10, 15] to deposit proteins in the form of the adjusted pattern, whereas

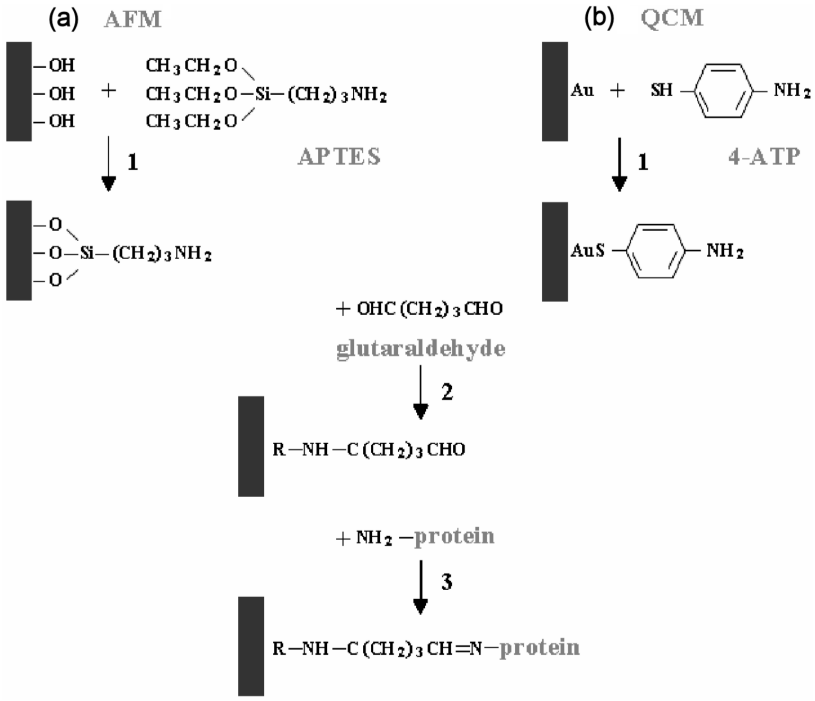

Fig. 1. Scheme of the immobilization procedures used for AFM and QCM experiments. 1. Silanization of the glass and gold surfaces using APTES (a) and 4-ATP (b), respectively. 2. Glutaraldehyde activation through the first one-step Schiffs base reaction with the amine-groups of modified substrates. 3. Protein deposition using the same Schiffs base reaction between the protein amine-groups and aldehyde groups of the substrates. R denotes $O_3Si(CH_2)_3$ in AFM and AuS-C_6H_4 in QCM.

quartz crystals were immersed in the protein solution for 30 min. In order to block the unbound aldehyde groups the substrates were rinsed with BSA solution (2.5 μM) and next with pure TBS.

2.3. Cantilevers functionalization

Commercially available silicon nitride cantilevers with a spring constant of 0.03 N/m (MLCT-AUHW, from Veeco) were used. They were functionalized with carboxypeptidase Y (2.5 μM). The procedure of silicon surface functionalization was the same as described above for a glass surface and has been already successfully used for AFM tip modification [10, 18].

2.4. Atomic force microscopy

A home-built atomic force microscope [19] was used to measure the interaction force between proteins. Force–distance curves were recorded at different retraction velocities ranging from 0.2 to 1.7 μm/s. The unbinding force was determined as a function of loading rate defined as a product of scanner velocity and the

system's spring constant. The system's spring constant k_s reflects the elasticity of both the cantilever and the molecular complex system. It was determined from the slope of the force versus displacement relationship of the retract curve [20] and its values were in the range of 0.005–0.007 N/m. Finally, the calculated loading rate r_f range varied from 1000 pN/s to 12000 pN/s. Several hundreds of force–distance curves (300–500) were recorded for each loading rate. All measurements were carried out in a TBS buffer (pH = 7.6) in the presence of metal ions, at room temperature.

2.5. Quartz crystal microbalance

A research quartz crystal microbalance (RQCM, Maxtek Inc.) was used. It allowed simultaneous measurements of crystal frequency (permitting one to estimate the mass of deposited proteins) and resistance (permitting an estimation of viscous losses of the layer). The frequency and mass resolutions were in the order of hundredths of hertz and tenths of nanograms per square centimetre, respectively. The RQCM was equipped with a phase-lock oscillator specifically tailored for measurements in liquid.

The quartz crystals (5 MHz AT-cut crystal with the Ti/Au electrodes) were purchased from Maxtek Inc. The surface of the electrodes was modified with proteins (Con A or BSA, 2.5 μM) according to the protocol described in Sect. 2.2. Next, the protein-modified quartz crystal was placed in a liquid cell setup. It was placed in such a way that only one gold electrode was in contact with the studied solution. Afterwards, a solution of CaY was added. Several different concentrations of CaY were used.

Two teflon tubes enabled the exchange of the buffer. All measurements were performed in a TBS buffer (pH = 7.6) in the presence of metal ions at room temperature. The temperature was monitored continuously during each measurement.

2.6. Fluorescence microscopy

Fluorescence microscopy was used in parallel with AFM for the identification of the produced patterns of proteins (Con A-FITC). The fluorescence images were performed using an Olympus BX51 equipped with a 100 W mercury lamp.

3. Results

3.1. Force spectroscopy

Prior to force spectroscopy measurements, the spatial distribution of studied proteins on the micro-sized area was made via molecular patterning. Protein stamping was carried out using the PDMS stamps with the micro-pattern [10, 15]. The receptor molecule (concanavalin A), specific to the mannose type ligands present on carboxypeptidase Y, was deposited using microcontact printing (μCP) [10, 15], while BSA protein, having no specificity to the selected ligand, was

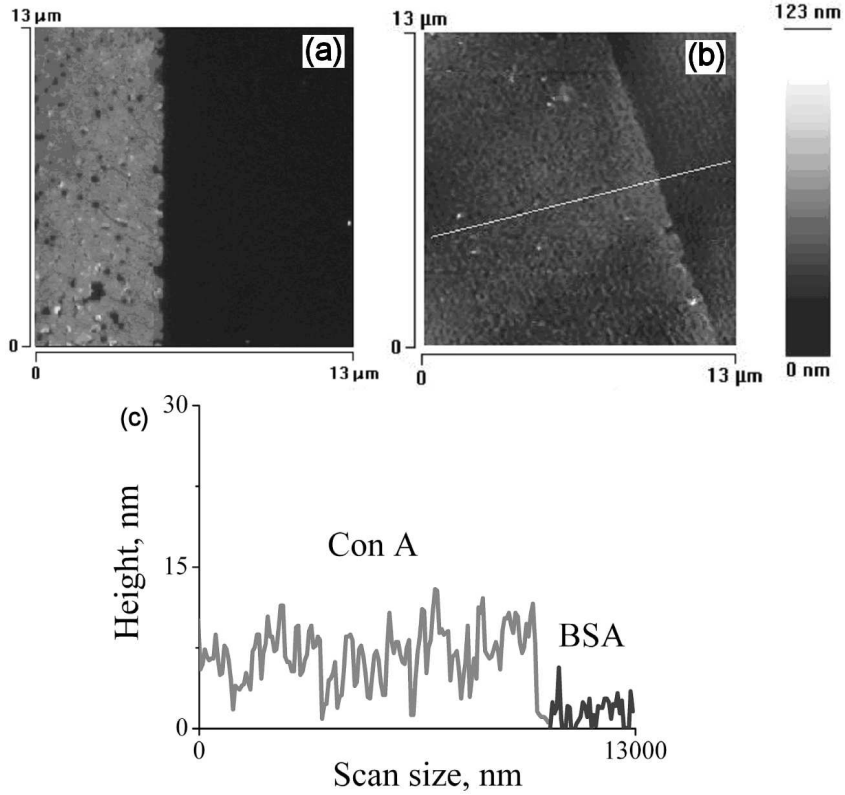

Fig. 2. The image of the surfaces of protein patterns (Con A–BSA) measured with fluorescence (a) and atomic force (b) microscopes. (a) The light-grey colour showed the region with deposited Con A labeled with FITC. The black colour corresponded to BSA-modified surface. (b) The AFM image of Con A/BSA modified surface and (c) its corresponding cross-section.

immobilized from the solution in the regions free of Con A (Fig. 2a,b). The surfaces patterned with Con A and BSA were imaged using fluorescence microscopy (Fig. 2a) and AFM (Fig. 2b) in parallel.

Both fluorescence and AFM images displayed the pattern of two protein layers. The average heights of both layers were determined from the cross-section of the AFM image. The thickness of the Con A layer was 7 ± 3 nm, while that for BSA layer was 3 ± 2 nm. The dimensions of a single Con A tetramer and a single BSA molecule are $6.7 \times 11.3 \times 12.2$ nm [21] and $4 \times 4 \times 14$ nm [22], respectively. Thus, the measured heights of protein layers indicate the presence of single molecular layers of Con A and BSA on the surface.

Using the substrates with protein patterns, the force spectroscopy measurements were performed. The recorded force–distance curves were analyzed in search of specific interaction between proteins following the method described partially

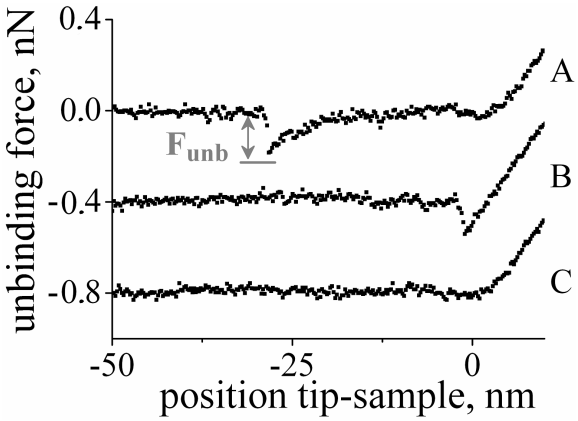

Fig. 3. Retract part of typical force–distance curves recorded for the interaction occurring between: curve A — Con A and CaY, curves B, C — BSA and CaY.

in [10]. Briefly, it was suggested that if distinct molecules were put in some specific order on a micro-areas of surface, then the force spectroscopy data obtained from such a prepared substrate would be spatially separated in the same order, which would facilitate the selection of the correct data. Another criterion applied was to analyze the retract part of the selected curves since it differs significantly depending on the type of molecular interaction occurring between the tip and the surface (specific or non-specific). The curves with the adhesion peaks characteristic of specific interaction (Fig. 3, curve A) were observed during the unbinding of a Con A–CaY complex. The formation of a molecular complex between two molecules, specific to each other, involves several types of intermolecular interactions (e.g. electrostatic attraction, hydrogen bonding, dispersion interaction, hydrophobic forces). Therefore the adhesive peaks observed while unbinding such a complex molecular system reveals a slow nonlinear increase in force versus increase in tip–sample separation (see Fig. 3, curve A).

To verify the specificity of Con A–CaY interaction another set of force–distance curves was obtained from the BSA-covered regions using the same AFM probe covered with CaY in the same measurement cycle. Some of curves showed the adhesion peaks characteristic of non-specific forces (Fig. 3, curve B) and some of them showed no rupture point at all indicating no interaction (Fig. 3, curve C) between the molecules. However, while BSA–CaY was unbinding no curves typical of a specific interaction were obtained. This result verifies that the above studied Con A–CaY interaction has a specific character.

Since the force–distance curves recorded for BSA–CaY interaction had the different character than that for Con A–CaY interaction, they were used as reference. The force–distance curves obtained for BSA–CaY complex unbinding were denoted as those typical of a non-specific interaction. Random force–distance curves of this type found in the Con A–CaY datasets were omitted.

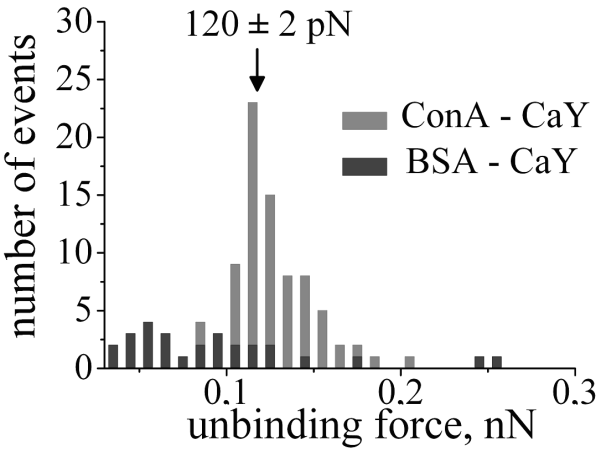

Fig. 4. The force distributions of the unbinding events obtained for Con A–CaY (grey bars) in the presence of metal ions and for BSA–CaY (dark grey bars).

The unbinding force values were obtained from the analysis of the retracting part of force–distance curves (recorded at a retraction velocity of 0.6 μm/s). Only the force–distance curves with the single adhesion peaks were taken into consideration. Figure 4 presents the unbinding force distribution for studied Con A–CaY (grey bars) and BSA–CaY (dark grey bars) pairs of molecules. A Gaussian function was fitted to the histogram obtained for the interaction between concanavalin A and carboxypeptidase Y proteins. The most probable unbinding force (i.e. its average value) was of 120 ± 2 pN (standard error of the mean).

3.2. Dynamic force spectroscopy

A theoretical description of the force-induced dissociation of a ligand–receptor complex has been proposed by Bell [23]. The unbinding pathway involves overcoming of single or multiple activation energy barriers. Bell postulated that the applied external force f decreases the energy barrier height leading to the exponential increase in the dissociation rate

$$k_{\mathrm{diss}}(f) = k_{\mathrm{diss}} \exp\left(\frac{f r_0}{kT}\right), \tag{1}$$

where k is the Boltzmann constant, T is temperature in K, k_{diss} is an intrinsic dissociation rate and r_0 is a position of the transition state. These parameters govern the dissociation kinetics of molecular complex under the applied force. Based on the Bell model, the relationship between the most probable unbinding force f^* needed to separate a single molecular complex and the applied loading rate has been deduced by Evans and Ritchie [5]:

$$f^* = \frac{kT}{r_0} \ln\left(\frac{r_f}{k_{\mathrm{diss}} kT/r_0}\right), \tag{2}$$

where r_f denominates the loading rate describing the rate of changing of the ap-

plied external force f. Thus, by measuring the unbinding force as a function of loading rate both parameters k_{diss} and r_0 can be estimated.

The dynamic force spectroscopy measurements of the unbinding forces were carried out for the force-induced dissociation between Con A and CaY molecules. The loading rates varied in a range of 1000–12000 pN/s. The representative histograms (100 events per histogram) obtained for different loading rates are presented in Fig. 5a. Maxima of the force distributions were attributed to the most probable forces causing bond unbinding.

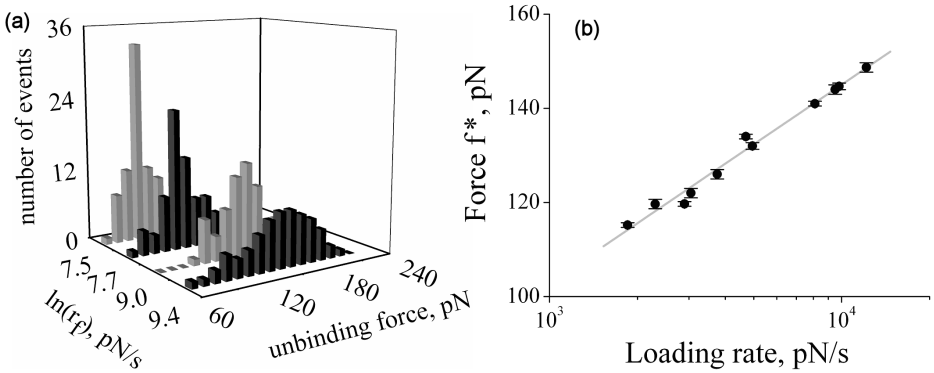

Fig. 5. (a) Force distribution obtained for unbinding of a Con A–CaY pair measured for different loading rate values. (b) The observed linear dependence between the most probable unbinding force f^* and the loading rate r_f. The plotted f^* are the mean values of the force obtained in five independent experiments (± standard deviation).

The obtained values of the most probable unbinding force causing Con A–CaY bond breakage were plotted against the corresponding values of the loading rates (Fig. 5b). From this plot, the parameters characterizing the dissociation of a single Con A–CaY complex were determined via fitting Eq. (2) to the data. The dissociation rate constant k_{diss} was determined to be 0.170 ± 0.060 s^{-1} and the position of the energy barrier r_0 was found to be 2.29 ± 0.04 Å.

3.3. Quartz microbalance measurements

In the QCM experiments the quartz crystal, covered with Con A, was placed in a liquid cell. Next, the CaY solution was added. The change of the resonant frequency was recorded as a function of time using QCM. A series of measurements were carried out for several different CaY concentrations ranged from 0.1 to 5 μM. The typical real-time frequency response curves recorded during CaY binding to Con A are presented in Fig. 6a. Knowing that the change of resonant frequency of the quartz crystal is proportional to the change of mass deposited on its surface [24], the larger frequency decrease obtained for 2.5 μM concentration of CaY was attributed to the larger mass deposition on the electrode of QCM.

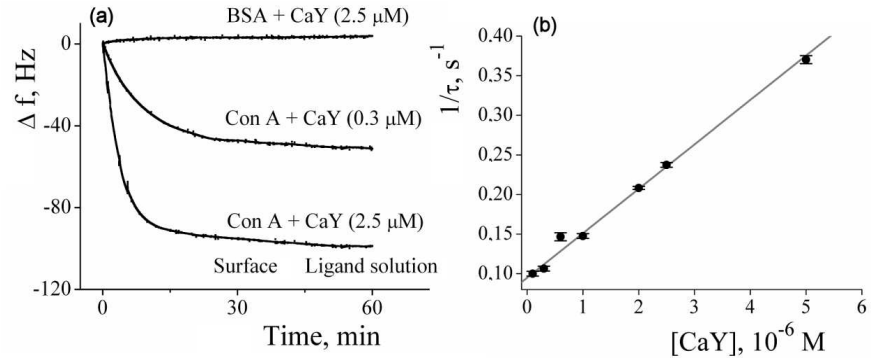

Fig. 6. (a) Frequency shift Δf as a function of time measured for adsorption of CaY (0.3, 2.5 μM) on the electrode surface modified with Con A and BSA. Measurements were performed in TBS containing Mn, Ca, and Mg ions. (b) The linear dependence between the relaxation constant and corresponding CaY concentration fitted with Eq. (4). The correlation coefficient of the fit was 0.994. The plotted data are average values of three independent experiments.

In the control measurement, the electrodes of quartz crystals were covered with BSA (2.5 μM) and CaY solutions of different concentrations were added. Bovine serum albumin protein was chosen since it shows no specificity to CaY. The resonance frequency curve corresponding to the control measurement with the largest used ligand concentration (2.5 μM) showed no frequency change (Fig. 6a) and consequently, it indicated no mass deposition on the electrode surface and no interaction between BSA and CaY.

Unlike in the gas phase and vacuum, in liquid solutions the resonant frequency is affected by both mass and liquid loading [25]. The visco-elasticity changes occurring on the quartz surface and the changes of the solution viscosity and density could cause loss of the mechanical energy dissipated in the medium. The motional resistance can be used to monitor such dissipation [26, 27]. Therefore, to make sure that during our experiment the change of resonant frequency was mainly affected by the deposited mass, the motional resistance (ΔR) was measured as a function of time. For the specific adsorption of CaY (5 μM) on a Con A-covered electrode only a small change of motional resistance ($\Delta R \approx 3.5\ \Omega$) was observed. Hence, it was assumed that the frequency change is proportional to the deposited mass and directly reflects the applied ligand concentration.

The reaction kinetic for Con A–CaY binding was studied in two steps. First, the measurements of the frequency response as a function of time using seven different concentrations of added ligands (0.1, 0.3, 0.6, 1.0, 2.0, 2.5, 5.0 μM CaY) were carried out. The following relation was applied to process the obtained data [7–9]:

$$\Delta f_t = \Delta f_{\max}\left(1 - \mathrm{e}^{-t/\tau}\right), \tag{3}$$

where Δf_t is the frequency change measured in the moment t, $\Delta f_{\max}$ is a value

of frequency at the end of measurement when all ligand molecules have bound to the surface, τ is a relaxation time.

By fitting Eq. (3) to the frequency response curve, the relaxation rate constant τ^{-1} can be obtained. The relaxation rate constant τ^{-1} is related to the initial ligand concentration C_{ligand} as

$$\tau^{-1} = k_{\text{ass}} C_{\text{ligand}} + k_{\text{diss}}. \tag{4}$$

The dissociation k_{diss} and association k_{ass} rate constants of Con A–CaY binding reaction were determined via fitting Eq. (4) to the dependence between the relaxation rate constants and corresponding initial concentration of CaY (Fig. 6b). The obtained rate constants were $k_{\text{diss}} = 0.095 \pm 0.002$ s^{-1} and $k_{\text{ass}} = (5.6 \pm 0.1) \times 10^4$ M^{-1} s^{-1}. The association equilibrium constant, $K_{\text{a}} = k_{\text{ass}}/k_{\text{diss}}$, was $(0.59 \pm 0.01) \times 10^6$ M^{-1}.

4. Discussion

The binding/unbinding between molecules can be studied using a wide spectrum of analytical methods. Among them, there are QCM and AFM, two techniques that are not yet widely used. They still need to be developed with respect to methodology and data analysis. The first method describes the binding/unbinding of molecules on a large scale giving both the association and dissociation parameters [28, 29]. The latter one enables studying of not only the unbinding of molecules but also provides local information at the level of single molecule interaction [30–32]. Both AFM and QCM can be successfully applied for quantitative description of the binding/unbinding process since the determined rates of reaction and equilibrium constants are intrinsic characteristics of a given interaction occurring between two types of molecules.

TABLE

The parameters describing the interaction between Con A–CaY molecules obtained using both force spectroscopy (AFM) and QCM techniques.

Method	Dissociation rate constant	Additional parameters
QCM	$k_{\text{diss}} = 0.095 \pm 0.002$ s^{-1}	$K_{\text{a}} = (0.59 \pm 0.01) \times 10^6$ M^{-1} $k_{\text{ass}} = (5.60 \pm 0.10) \times 10^4$ M^{-1} s^{-1}
AFM	$k_{\text{diss}} = 0.170 \pm 0.060$ s^{-1}	$r_0 = 2.29 \pm 0.04$ Å

In the present work, the results of AFM and QCM measurements performed for the interaction occurring between concanavalin A and carboxypeptidase Y were compared. The parameters describing the binding/unbinding between these protein molecules were determined (see Table). The common parameter for both techniques is a dissociation rate constant. Its value obtained for Con A–CaY was comparable for AFM and QCM: $k_{\text{diss}} = 0.170 \pm 0.060$ s^{-1} and $k_{\text{diss}} = 0.095 \pm 0.002$ s^{-1}.

From QCM measurements, the association rate and the association equilibrium constants (k_{ass}, K_{a}) were also obtained. The obtained K_{a} value is comparable with that presented elsewhere ($K_{\mathrm{a}} = 0.1{-}3 \times 10^6$ M^{-1} [33]; $K_{\mathrm{a}} = 1.7 \times 10^6$ M^{-1} [14]; $K_{\mathrm{a}} = 0.3 \times 10^6$ M^{-1} [34]).

The force spectroscopy mode of AFM enables one also to explore the energy landscape of dissociation pathway from the low-energy (bound complex) to the high-energy states (unbound) through the transition state. From the force spectroscopy measurement the number of the energy barriers and the positions of corresponding transition states with respect to the energy minimum are determined. The energy landscape of Con A–CaY dissociation was constructed (Fig. 7) using the determined value of transition state position (2.29 ± 0.04 Å) and the equilibrium K_{a} constant obtained from QCM experiment. The K_{a} value was utilized to estimate the free energy $\Delta G = 13.3kT$, corresponding to the height of the energy barrier ($\Delta G = -kT \ln K_{\mathrm{a}}$).

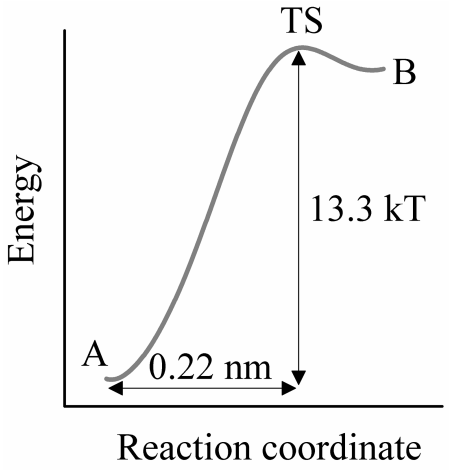

Fig. 7. The illustration of the energy landscape of Con A–CaY dissociation. A simple two-state model consisting of bound (A) and unbound (B) states is presented. The dissociation pathway proceeds via one transition state. The energy barrier height was estimated using the equilibrium constant delivered from QCM. The position of the transition state was obtained from the force spectroscopy (AFM) measurements.

As regards the number of energy barriers, the presence of one linear region on the plot of the most probable unbinding force versus the logarithm of the applied loading rate suggests the presence of one energy barrier in the energy landscape of explored unbinding reaction [5]. Moreover, for some molecular complexes several linear regions can be observed ([20, 31] and [32]). In such a case, the presence of sequential energy barriers is suggested with the corresponding values of dissociation rates and transition states positions.

The presented results revealed only one barrier in the energy landscape of Con A–CaY complex dissociation. However, the range of applied loading rates was not as wide as that used in the other works ([20, 31] and [32]). If the range of used loading rates is not sufficiently wide then the energy landscape is only partially explored, as only one energy barrier can be observed [5]. However, the applied values of loading rate (low range) enabled the investigation of the outermost barrier properties. This case is close to the dissociation without application of the external force. Therefore, the rate constant of the dissociation over the outermost energy barrier obtained from the force spectroscopy measurements should be comparable to that measured in solution using other techniques such as SPR, ELISA, or QCM.

5. Conclusions

The results presented here have shown that both techniques (atomic force microscopy working in force spectroscopy mode and quartz crystal microbalance) can be successfully applied in simultaneous and complementary studies of a chosen molecular interaction. The same methods of sample preparation permit the direct comparison between the data obtained via AFM and QCM.

They gave comparable values of dissociation rate constants and several additional parameters distinctive for the studied interaction, such as association rate and association equilibrium constants and a position of transition state.

Acknowledgments

This work was partially supported by the Swiss National Science Foundation and its NCCR "Nanoscale Science" and by the 6FP EU project No. MRTN-CT-2003-503923 (CELLION).

References

[1] J. Homola, *Anal. Bioanal. Chem.* **377**, 528 (2003).

[2] D. Monroe, *Anal. Chem.* **56**, 920A (1984).

[3] I.M. Chaiken, *J. Chromatogr.* **376**, 11 (1986).

[4] R.J. Linhardt, T. Toida, *Science* **298**, 1441 (2002).

[5] E. Evans, K. Ritchie, *Biophys. J.* **72**, 1541 (1997).

[6] R. Merkel, P. Nassoy, A. Leung, K. Ritchie, E. Evans, *Nature* **397**, 50 (1999).

[7] Y. Mao, W. Wei, D. He, L. Nie, S. Yao, *Anal. Biochem.* **306**, 23 (2002).

[8] Y. Okahata, K. Niikura, H. Furusawa, H. Matsuno, *Anal. Sci.* **16**, 113 (2000).

[9] J. Hu, D. Yang, Q. Kang, D. Shen, *Sensor Actuat. B* **96**, 390 (2003).

[10] K. Lebed, G. Pyka-Fosciak, J. Raczkowska, M. Lekka, J. Styczeń, *J. Phys., Condens. Matter* **17**, S1447 (2005).

[11] K. Lebed, A. Kulik, L. Forró, M. Lekka, *J. Colloid. Interf. Sci.* **299**, 41 (2006).

[12] E. Song, *Hepatol. Res.* **26**, 311 (2003).

[13] D. Stewart, J. Forrest, W. Muller, *Biotechnol. Adv.* **14**, 553 (1996).

[14] M. Mizuno, M. Noguchi, M. Imai, T. Motoyoshia, T. Inazu, *Bioorg. Med. Chem. Lett.* **14**, 485 (2004).

[15] A. Bernard, E. Delamarche, H. Schmid, B. Michel, H.R. Bosshard, H. Biebuyck, *Langmuir* **14**, 2225 (1998).

[16] B. Agrawal, I. Goldstein, *Biochim. Biophys. Acta* **147**, 262 (1967).

[17] S. Si, L. Si, F. Ren, D. Zhu, Y. Fung, *J. Colloid Interf. Sci.* **253**, 47 (2002).

[18] P.F. Luckham, K. Smith, *Faraday Discuss.* **111**, 307 (1998).

[19] M. Lekka, J. Lekki, A. Shoulyarenko, B. Cleff, J. Stachura, Z. Stachura, *Pol. J. Pathol.* **47**, 51 (1996).

[20] C. Yuan, A. Chen, P. Kolb, V.T. Moy, *Biochemistry* **39**, 10219 (2000).

[21] J. Bouckaert, F. Poortmans, L. Wyns, R. Loris, *J. Biol. Chem.* **271**, 16144 (1996).

[22] A.K. Wright, M.R. Thompson, *Biophys. J.* **15**, 137 (1975).

[23] G.I. Bell, *Science* **200**, 618 (1978).

[24] G.Z. Sauerbrey, *Z. Phys.* **155**, 206 (1959).

[25] K.K. Kanazawa, J.G. Gordon, *Anal. Chim. Acta* **175**, 99 (1985).

[26] S.J. Martin, V.E. Granstaff, G.C. Frye, *Anal. Chem.* **63**, 2272 (1991).

[27] H. Muramatsu, E. Tamiya, I. Karube, *Anal. Chem.* **60**, 2142 (1988).

[28] A. Janshoff, H.J. Galla, C. Steinem, *Angew. Chem. Int. Ed.* **39**, 4004 (2000).

[29] K.A. Marx, *Biomacromolecules* **4**, 1099 (2003).

[30] F. Schwesinger, R. Ros, T. Strunz, D. Anselmetti, H.-J. Guntherodt, A. Honegger, L. Jemutus, L. Tiefenauer, A. Pluckthun, *Proc. Natl. Acad. Sci. USA* **97**, 9972 (2000).

[31] X. Zhang, E. Wojcikiewicz, V.T. Moy, *Biophys. J.* **83**, 2270 (2002).

[32] F. Li, S.D. Redick, H.P. Erickson, V.T. Moy, *Biophys. J.* **84**, 1252 (2003).

[33] R.G. Gallego, S.R. Haseley, V.F.L. Van Miegem, J.F.G. Vliegenthart, J.P. Kamerling, *Glycobiology* **14**, 373 (2004).

[34] D. Mislovicova, J. Masarova, J. Svitel, R. Mendichi, L. Soltes, P. Gemeiner, B. Danielsson, *Bioconj. Chem.* **13**, 136 (2002).